Identification of weld sub-surface defects by radiographic images using texture features

E V Ramana[1], *Sai* Varun Penekalapati[1], *Kiran* Kumar Namala[1*]

[1]Mechanical Engineering Department, VNR Vignana Jyothi Institute of Engineering and Technology Hyderabad, Telangana, India

Abstract. Non-Destructive Testing (NDT) is important to detect sub-surface defects in the weldments to ensure the quality of weld joints. The weld radiographs are digitized using a high-resolution digital camera. Data augmentation techniques are applied to expand the radiographic image dataset. Multi-class defect classification is done using the Gray-level co-occurrence matrix as a feature extractor and these features are given as input to various classifiers for classifying slag inclusion, incomplete penetration, and acceptable weld bead classes. The proposed methodology achieved the highest accuracies of 84%,83%,80%,70%, and 64% respectively for GLCM plus Random Forest, GLCM plus XGBoost, GLCM plus lightGBM, GLCM plus KNN, and GLCM plus SVM. The technology of applying ML techniques on radiographic images in detection of defects in welding as well as other manufacturing processes can be a sustainable practice.

Keywords: Gray level co-occurrence matrix, LightGBM, Support vector machine, Random Forest, non-destructive testing.

1 Introduction

Welding plays a key role in many sectors like the shipping industry, aerospace, land transportation, petrochemical, and chemical plants. Failures in incorporating proper practices while welding may give rise to weld defects. Non – destructive testing can be used to detect sub-surface defects of the weldments to make them more reliable.

Manual weld inspection is only 80% effective, and this is achieved when stringent inspection checks are carried out (Shafeek et al., 2004). Non-destructive testing is a cost-effective method to ensure the weld quality meets the design standards and operational requirements (Rathod et al., 2012). The radiographic technique is employed to detect sub-surface flaws without damaging the part being inspected.

A Gray level co-occurrence matrix is used for the texture analysis of an image (Sebastian et al., 2012). Kumar et al. (2014) performed multiclass classification using the ANN classifier and features are drawn from the GLCM matrix. Mery and Berti (2003) used 2D Gabor

* Corresponding Author: kirankumar_n@vnrvjiet.in

functions and Gray level co-occurrence matrix to extract texture-based features. Mall et al. (2019), used GLCM to extract texture features from the radiographic images of bones and to classify them into no fracture and fracture classes. Linear SVM, decision tree, logistic regression, and LBF SVM are used as classifiers. Patil and Reddy (2021) incorporated pre-processing techniques to enhance image quality. Further,10 texture features are extracted using GLCM. Finally, SVM and ANN are used as classifiers. Tou et al. (2007) observed a decrease in the decision rate while working with more than six features. An increase in features also affects the computation time. Mohanaiah et al. (2013) showed that for good image resolution and least information loss 128 x128 size images are optimal. Da Silva et al. (2004) stated that the quality of features is more important than the quantity of features for a classifier to classify the images. Haralick et al. (1973) discussed the various applications of textural-based features for image classification. Based on the literature review performed, six features are selected for avoiding any decrease in accuracy and for an efficient computation time. In the current work, the texture descriptors extracted from Gray-Level Cooccurrence Matrix by varying the directions and spatial pixel distances are given as input for the multiclass classification.

2 Methodology

The block diagram of the methodology implemented in the extraction of features from the radiographic images of the weldments and classification of the sub-surface defects is shown in Figure.1.

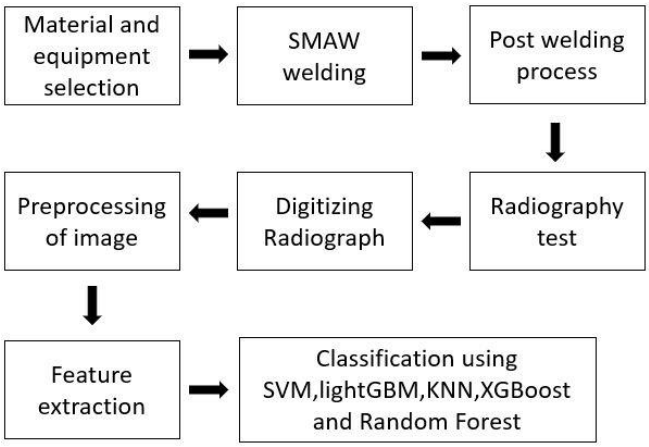

Fig. 1. Methodology

2.1 Material and equipment selection

Mild steel (MS) AISI 1019 plates of size 150X50X6mm are used to prepare the weld specimens by shielded metal arc welding employing an arc welding transformer with 3-phase AC/DC power supply and E6013 electrodes in the present work.

2.2 SMAW welding

Shielded metal arc welding is used in the present work and weld parameters are varied to induce the lack of penetration and slag inclusion defects in the weld specimens by altering the weld current. The lack of penetration in the welded specimens is induced by applying the

current in the range of 65-75A and maintaining a constant voltage of 415V. The slag inclusion in the specimens is created by the damped electrode. The acceptable specimens are prepared by maintaining the current in the range of 115-125A and a constant voltage of 415V.Fifteen weld specimens are prepared for each class (Acceptable, slag inclusion, and lack of penetration).

2.3 Post-welding process

The weld bead is cleaned with an abrasive cloth of various grit sizes. The unwanted particles are removed from the weld surface using a microfiber cloth.

2.4 Radiography test

Sub-surface defect identification is done by performing a radiography test on the weld specimens to acquire the radiographic images.

2.5 Digitizing radiographic images

A high-resolution camera is used to capture the radiographic images of weld specimens under suitable lighting conditions. Sample radiographic images of acceptable weld bead and sub-surface defects are shown in Figure 2.

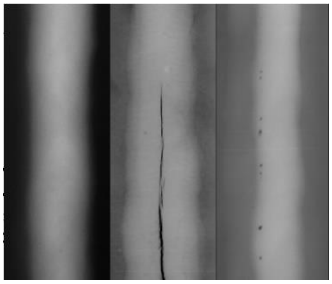

(a) (b) (c)

Fig. 2. Sample radiographic images a) Acceptable weld bead b) lack of penetration c) Slag inclusion

2.6 Pre-processing of images

The regions of interest are cropped from each image and each image is converted into a single channel (grayscale) image. Then, each digitized image is cropped into three parts to increase the size of the image dataset by acquiring 45 images for each class. Later, each image is resized to 128x128 to minimize the loss of information. The synthetic images are generated by applying data augmentation techniques like random zooming, flipping, rotation, shift, and shear operations to increase the size of the dataset.

The final radiographic weld image dataset comprises 1188 images of which 80% are used for training and the remaining 20% are utilized for testing.

2.7 Feature extraction

Gray Level Co-occurrence Matrix (GLCM) is a second-order statistical method that establishes a relationship between a pair of pixels at a time. i.e., the reference and neighboring

pixel for the analysis of texture. Texture features are extracted using the GLCM matrix and subsequent application of texture descriptors like Energy, contrast, correlation, homogeneity, dissimilarity, and entropy in the current work.

2.8 Classification using SVM, light GBM, KNN, XGBoost and Random Forest

The extracted texture features of the weld images are given as input to light GBM, Random Forest, SVM, XG Boost and KNN for classification of acceptable weld bead, slag inclusion, and lack of penetration. Two experiments are conducted by varying the pixel distance and changing the directions to classify the dataset into three classes using the classifiers mentioned. A comparative study is done between the classifiers based on these two experiments.

For light GBM, Gradient-based One Side Sampling is used as a hyperparameter, and the learning rate is set as 0.05. The Random state value and decision trees are set as 10, and 100 respectively for the random forest classifier. The hyperparameters for the learning rate and decision trees are set as 0.3 and 100 respectively for XGBoost. One-vs-one hyperparameter is implemented for multiclass classification in SVM classifier. The number of clusters is set to 10 for the KNN classifier.

3 Results and Discussion

3.1 Experiment 1

In the 1st experiment, six second-order texture features (contrast, homogeneity, energy, correlation, entropy, and dissimilarity) are extracted in two different directions i.e.,0º and 180º. A spatial pixel distance(d) is taken as 2 in this experiment. Therefore, a total of 6x2=12 texture descriptors are utilized for extracting features of radiographic images.

Then, the extracted features are given as input to various classifiers (KNN, SVM, lightGBM, XGBoost, and Random Forest) for the multi-class classification of radiographic images.

GLCM plus SVM, GLCM plus KNN, GLCM plus lightGBM, GLCM plus XGBoost, GLCM plus Random Forest classifiers achieved prediction accuracies of 64%,70%,75%,77% and 79% respectively.

3.1.1. Confusion matrices of ML models for 1st experiment

The confusion matrices of GLCM plus SVM, GLCM plus KNN, GLCM plus lightGBM, GLCM plus XGBoost, and GLCM plus Random Forest are shown in figures 3 to 7 respectively.

0- Acceptable weld joint

1- Incomplete penetration

2- Slag Inclusion

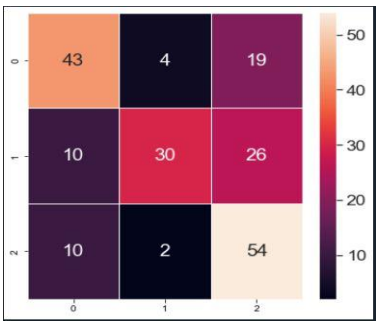

Fig.3. Confusion matrix of GLCM plus SVM (1st experiment)

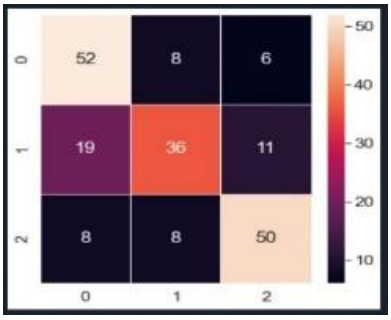

Fig.4. Confusion matrix of GLCM plus KNN (1st experiment)

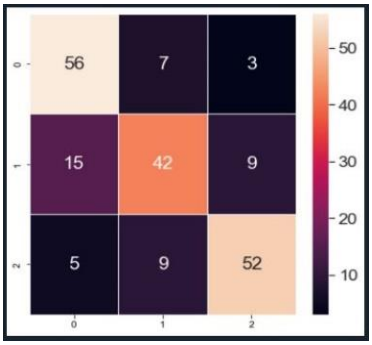

Fig.5. Confusion matrix of GLCM plus lightGBM (1st experiment)

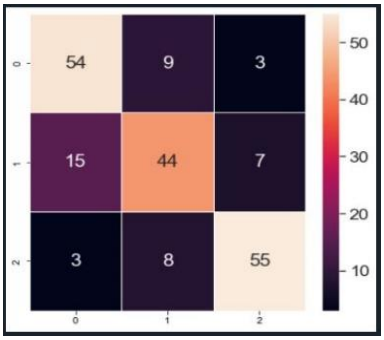

Fig.6. Confusion matrix of GLCM plus XGBoost (1st experiment)

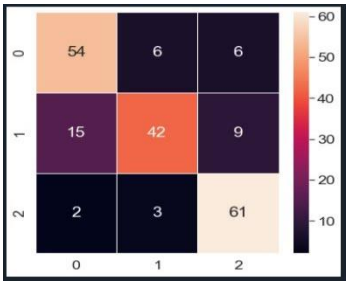

Fig.7. Confusion matrix of GLCM plus Random Forest (1st experiment)

3.1.2.Precision, recall, and F-1 score for ML models (1st experiment)

The Precision, recall, and F-1 score for ML models of GLCM plus SVM, GLCM plus KNN, GLCM plus lightGBM, GLCM plus XGBoost, and GLCM plus Random Forest for 1st experiment are presented in Tables 1 to 5 respectively.

Table 1. Precision, recall, and F-1 score of GLCM plus SVM (1st experiment)

Class	**GLCM plus SVM (1st experiment)**			
	Precision	**Recall**	**F-1**	**Support**
Acceptable bead	0.68	0.65	0.67	66
Incomplete penetration	0.83	0.45	0.59	66
Slag Inclusion	0.55	0.82	0.65	66

Table 2. Precision, recall, and F-1 score of GLCM plus KNN (1st experiment)

Class	**GLCM plus KNN (1st experiment)**			
	Precision	**Recall**	**F-1**	**Support**
Acceptable bead	0.66	0.79	0.72	66
Incomplete penetration	0.69	0.55	0.61	66
Slag Inclusion	0.75	0.76	0.75	66

Table 3. Precision, recall, and F-1 score of GLCM plus lightGBM (1st experiment)

Class	**GLCM plus lightGBM (1st experiment)**			
	Precision	**Recall**	**F-1**	**Support**
Acceptable bead	0.74	0.85	0.79	0.66
Incomplete penetration	0.72	0.64	0.68	0.66
Slag Inclusion	0.81	0.79	0.80	0.66

Table 4. Precision, recall, and F-1 score of GLCM plus XGBoost (1st experiment)

Class	GLCM plus XGBoost (1st experiment)			
	Precision	**Recall**	**F-1**	**Support**
Acceptable bead	0.75	0.82	0.78	66
Incomplete penetration	0.72	0.67	0.69	66
Slag Inclusion	0.85	0.83	0.84	66

Table 5. Precision, recall, and F-1 score of GLCM plus Random Forest (1st experiment)

Class	GLCM plus Random Forest (1st experiment)			
	Precision	**Recall**	**F-1**	**Support**
Acceptable bead	0.76	0.82	0.79	66
Incomplete penetration	0.82	0.64	0.72	66
Slag Inclusion	0.80	0.92	0.86	66

3.2 Experiment - 2

In the 2nd experiment, 6 texture features same as 1st experiment are extracted for spatial pixel distances of 1,2,3, and 4 in four different directions (0º,45º,90º,135º). Therefore, 96 texture descriptors are extracted for each image. The features extracted from GLCM are given as input to the classifiers, the same as in experiment 1.

GLCM plus Random Forest, GLCM plus XGBoost , GLCM plus lightGBM, GLCM plus KNN, and GLCM plus SVM exhibited the classification accuracies of 84%,83%,80%,65%,and 59% respectively.

3.2.1 Confusion matrix of ML models (2nd experiment)

The confusion matrices of GLCM plus SVM, GLCM plus KNN, GLCM plus XGBoost, GLCM plus lightGBM, and GLCM plus Random Forest are shown from figures 8 to12 respectively.

Fig. 8. Confusion matrix of GLCM plus SVM (2nd experiment)

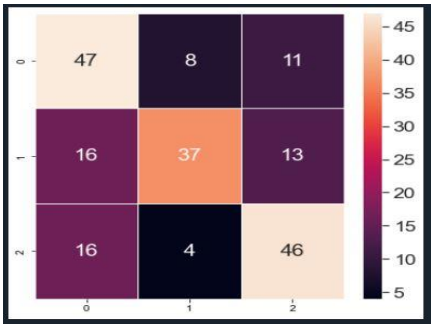

Fig. 9. Confusion matrix of GLCM plus KNN (2nd experiment)

Fig. 10. Confusion matrix of GLCM plus XGBoost (2nd experiment)

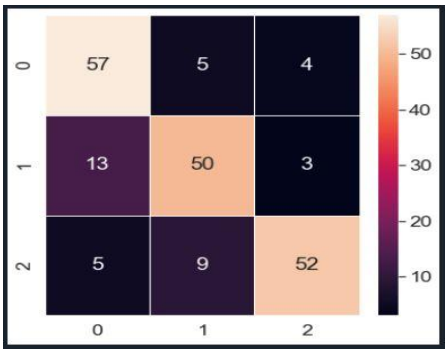

Fig. 11. Confusion matrix of GLCM plus lightGBM (2nd experiment)

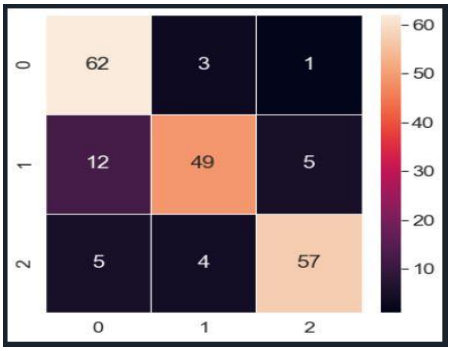

Fig.12. Confusion matrix of GLCM plus Random Forest 2nd experiment)

3.2.2 Precision, recall, and F-1 score for ML models (2nd experiment)

The Precision, recall, and F-1 score for ML models of GLCM plus SVM, GLCM plus KNN, GLCM plus lightGBM, GLCM plus XGBoost, and GLCM plus Random Forest for 2nd experiment are presented in Tables 6 to 10 respectively.

Table 6. Precision, recall, and F-1 score of GLCM plus SVM (2nd experiment)

Class	GLCM plus SVM (2nd experiment)			
	Precision	Recall	F-1	Support
Acceptable bead	0.56	0.67	0.61	66
Incomplete penetration	0.94	0.44	0.60	66
Slag Inclusion	0.51	0.68	0.58	66

Table 7. Precision, recall, and F-1 score of GLCM plus KNN (2nd experiment)

Class	GLCM plus KNN (2nd experiment)			
	Precision	Recall	F-1	Support
Acceptable bead	0.59	0.71	0.65	66
Incomplete penetration	0.76	0.56	0.64	66
Slag Inclusion	0.66	0.70	0.68	66

Table 8. Precision, recall, and F-1 score of GLCM plus XGBoost (2nd experiment)

Class	GLCM plus XGBoost (2nd experiment)			
	Precision	Recall	F-1	Support
Acceptable bead	0.79	0.91	0.85	66
Incomplete penetration	0.81	0.85	0.83	66
Slag Inclusion	0.94	0.76	0.84	66

Table 9. Precision, recall, and F-1 score of GLCM plus lightGBM (2nd experiment)

Class	GLCM plus lightGBM (2nd experiment)			
	Precision	Recall	F-1	Support
Acceptable bead	0.76	0.86	0.81	66
Incomplete penetration	0.78	0.76	0.77	66
Slag Inclusion	0.88	0.79	0.83	66

Table 10. Precision, recall, and F-1 score of GLCM plus Random Forest (2nd experiment)

Class	GLCM plus Random Forest (2nd experiment)			
	Precision	Recall	F-1	Support
Acceptable bead	0.78	0.94	0.86	66
Incomplete penetration	0.88	0.74	0.80	66
Slag Inclusion	0.90	0.86	0.88	66

4 Conclusions

The sub-surface weld defects and acceptable beads are identified from the radiographic images by extracting textural features through the gray level co-occurrence

matrix and applying KNN, SVM, lightGBM, Random Forest, and XGboost classifiers. Two experiments are conducted by varying the directions and spatial pixel distances of GLCM. In the 1st experiment, the prediction accuracies achieved by GLCM plus SVM, GLCM plus KNN, GLCM plus lightGBM, GLCM plus XGBoost, and GLCM plus Random Forest are 64%,70%,75%,77% and 79% respectively. In the 2nd experiment, the prediction accuracies achieved by GLCM plus SVM, GLCM plus KNN, GLCM plus lightGBM, GLCM plus XGBoost, and GLCM plus Random Forest are 59%,65%,80%,83%, and 84% respectively. GLCM plus Random Forest achieved the highest accuracy among both experiments. It is found that GLCM plus KNN and GLCM plus SVM performed better with a smaller number of features whereas, the rest of the hybrid machine learning algorithms achieved higher accuracies with a greater number of features. The texture features for radiographic imaging in the identification of weld sub-surface defects aligns with diverse sustainable practices to promote resource efficiency, energy conservation, lower environmental impact, enhanced durability, improved safety and optimized maintenance.

References

1. Shafeek, H. I., E. S. Gadelmawla, A. A. Abdel-Shafy, and I. M. Elewa. "Assessment of welding defects for gas pipeline radiographs using computer vision." NDT & e International 37, no. 4 (2004): 291-299.
2. Rathod, Vijay R., Radhey Shyam Anand, and Alaknanda Ashok. "Comparative analysis of NDE techniques with image processing." Nondestructive Testing and Evaluation 27, no. 4 (2012): 305-326.
3. Sebastian V, Bino, A. Unnikrishnan, and Kannan Balakrishnan. "Gray level co-occurrence matrices: generalisation and some new features." arXiv preprint arXiv:1205.4831 (2012).
4. Kumar, Jayendra, Radhey Shyam Anand, and S. P. Srivastava. "Multi-class welding flaws classification using texture feature for radiographic images." In 2014 International Conference on Advances in Electrical Engineering (ICAEE), pp. 1-4. IEEE, 2014.
5. Mery, Domingo, and Miguel Angel Berti. "Automatic detection of welding defects using texture features." Insight-Non-Destructive Testing and Condition Monitoring 45, no. 10 (2003): 676-681.
6. Mall, Pawan Kumar, Pradeep Kumar Singh, and Divakar Yadav. "GLCM based feature extraction and medical X-RAY image classification using machine learning techniques." In 2019 IEEE Conference on Information and Communication Technology, pp. 1-6. IEEE, 2019.
7. Patil, Rajesh V., and Y. P. Reddy. "An autonomous technique for multi class weld imperfections detection and classification by support vector machine." Journal of Nondestructive Evaluation 40, no. 3 (2021): 76.
8. Tou, Jing Yi, Yong Haur Tay, and Phooi Yee Lau. "Gabor filters and grey-level co-occurrence matrices in texture classification." In MMU International symposium on information and communications technologies, pp. 197-202. 2007.
9. Mohanaiah, P., P. Sathyanarayana, and L. GuruKumar. "Image texture feature extraction using GLCM approach." International journal of scientific and research publications 3, no. 5 (2013): 1-5.
10. Da Silva, Romeu R., Luiz P. Calôba, Marcio HS Siqueira, and Joao MA Rebello. "Pattern recognition of weld defects detected by radiographic test." NDT & e International 37, no. 6 (2004): 461-470.
11. Haralick, Robert M., Karthikeyan Shanmugam, and Its' Hak Dinstein. "Textural features for image classification." IEEE Transactions on systems, man, and cybernetics 6 (1973): 610-621.